Northumbria
University
NEWCASTLE

Low-cost wearable sensor based on a D-shaped plastic optical fiber for respiration monitoring

Yu-Lin Wang, Bin Liu*, Yi-Neng Pang, Juan Liu, Jiu-Lin Shi, Sheng-Peng Wan, Xing-Dao He, Jinhui Yuan** and Qiang Wu**

***Abstract*—A low cost, wearable textile-based respiratory sensing system is proposed and experimentally demonstrated. A highly sensitive D-shaped plastic optical fiber (POF) sensor that responds to bending is integrated into an elastic band structure to form a respiratory sensing system. The curvature sensing experiments were conducted on the D-shaped POF sensor, which has a coefficient of determination (R^2) of 0.9977. The system can be used to monitor not only the respiratory rate (RR) of the human body under different movement states (resting, walking and running), but also the RR of steady and unsteady respiratory signals due to different physiological states. In addition, using the proposed signal processing technique, the interference of motion noise can be removed and the influence of body movement on the sensor response can be eliminated. The advantages of the system are its low cost, compactness and simplicity in design. Thus, the application of the proposed respiratory sensing system provides a simple and inexpensive optical solution for wearable health.**

***Index Terms*—Optical fiber sensing, D-shaped plastic optical fiber, Respiration monitoring, Wearable device**

I. Introduction

BREATH is an important activity to maintain human physiological functions [1]. Analysis of the breath allows for early detection and post-treatment monitoring of many diseases such as head and neck cancer, lung cancer, and Alzheimer's disease [2-4]. RR is an important parameter of the respiratory function index and is the most important vital sign [5]. RR is an early predictor of clinical deterioration, cardiac arrest, and sepsis in children [6-8]. In order to meet the needs of modern clinical medicine and health monitoring, the measurement of RR has been increasingly studied in various fields.

Respiratory monitoring can be performed using two methods: contact methods, in which there is an instrument attached directly to a subject's body, and non-contact methods, in which the instrument is not attached [9]. For non-contact methods, one of the most promising methods is currently based on video signal processing techniques [10-12]. However, the main disadvantages are high cost, high computational effort and privacy conflicts. Therefore, the development of various sensor technologies appears in many studies of contact methods. For the contact methods, the main sensors used for respiratory monitoring are electronic sensors and optical sensors. Traditional electronic breath sensors are humidity sensors, strain sensors, pressure sensors, and heat and airflow sensors [13-16]. Compared with traditional electronic sensors, optical fiber sensor technique has many advantages in human health monitoring, such as the high sensitivity, resistence to corrosion and immunity to electromagnetic interference. Silicon optical fiber sensors are widely used in human respiratory monitoring, such as fiber optic grating sensor, Mach-Zehnder interferometer (MZI) structure, Multimode interferometer structure, singlemode-multimode-singlemode (SMS) and so on [17-23]. These silica fiber sensors are highly sensitive, but they are also costly. This is because they often use expensive light sources and measurement equipment. Further, the low-cost schemes have emerged, including micro-bend optical fiber sensor and hetero-core optical fiber sensor [24,25]. Whereas, micro-bend optical fiber sensors may cause poor comfortability due to their hard sensitization structure. Meanwhile, the silica optical fibers are prone to breakage, which poses a risk to the user and can lead to injury.

Recently, plastic optical fiber with better flexibility and wearability shows excellent application value in wearable devices for health monitoring [26]. In 2014, M. Krehel *et al.* presented a respiratory sensing system based on plastic optical fibers (POFs). The system not only measures RR, but also distinguishes between three respiratory types (diaphragmatic, upper costal and mixed) [27]. W. Zheng *et al.* introduced an intensity-based notched POF strain sensor for respiratory monitoring, and experimental results showed a strong correlation between the sensor and the clinical monitor [28]. In 2017, D. Sartiano *et al.* presented a low-cost plastic optical fiber pressure sensor, embedded in a mattress, that is suitable for monitoring respiratory movements [29]. In 2019, A. Aitkulov *et al.* proposed a sensing system based on the integration of a smartphone with POFs that extracts information about the

This work was jointly supported by National Natural Science Foundation of China (NSFC) (11864025, 62065013, 61465009); Natural Science Foundation of Jiangxi Province (Grant No. 20192ACB20031, 20192ACBL21051, 20202ACBL202002); Key R & D projects of Ministry of science and technology of China (Grant No. 2018YFE0115700). (Correspondence authors: Bin Liu, Jinhui Yuan and Qiang Wu)

Yu-Lin Wang, Bin Liu, Yi-Neng Pang, Juan Liu, Jiu-Lin Shi, Sheng-Peng Wan, Xing-Dao He and Qiang Wu are with Key Laboratory of Opto-Electronic Information Science and Technology of Jiangxi Province, Nanchang Hangkong University, Nanchang 330063, China (e-mail: wangyulinr@163.com; liubin_d@126.com; fuyaohonghu@126.com; 18042@nchu.edu.cn; jiulinshi@126.com; spwan@nchu.edu.cn; hxd@nchu.edu.cn; qiang.wu@northumbria.ac.uk). Qiang Wu is also with Faculty of Engineering and Environment, Northumbria University, Newcastle Upon Tyne NE1 8ST, UK.

Jinhui Yuan are with the Research Center for Convergence Networks and Ubiquitous Services, University of Science & Technology Beijing, Beijing 100083, China. (e-mail: yuanjinhui81@163.com).

periodicity of respiration in the time and frequency domains [30]. A. G. Leal-Junior *et al.* describe a POF sensor that simultaneously measures respiration and heart rate (HR) with an error of less than 4 breaths per minute for HR and 2 breaths per minute for RR, respectively [31]. However, these methods mentioned above have more or less disadvantages in terms of complex sensor structure, inconvenient use, relatively high cost or unavailability during human movement, *etc*.

In this paper, a low-cost, wearable textile-based respiratory sensing system is proposed. Respiratory monitoring can be achieved by using a D-shaped POF with side-polished structure. The sensor has advantages of simple structure, small size, easy to wear and easy to implant in clothes. The D-shaped POF sensor is fixed to the human abdomen through an elastic band, which can effectively monitor the RR of the human body under different breathing conditions.

II. D-SHAPED POF SENSOR SENSING PRINCIPLE

The Young's modulus of POF is low, ranging from 2-4 GPa, and its elastic limit is around 10%. Therefore, these characteristics indicate that POF has high elasticity, which is beneficial to strain monitoring of structures with inherently high compliance [32,33]. D-shaped POF sensor is made by removing some of the sides of the cylindrical fiber, which forms a sensitive zone to increase the sensitivity of the sensor and the linearity of the signal attenuation when the fiber is bending. For the D-shaped POF, the cladding and core material have been partially stripped and thus its Young's modulus is lower. This allows the POF sensors to exhibit higher inherent sensitivity [34]. Nowadays, the D-shaped POF is used in many applications, especially for human motion monitoring or as a joint goniometer [35,36]. The strength of the D-shaped POF is also sufficient for respiratory monitoring. R. Q. Liu *et al.* proposed a bend-enhanced curvature POF sensor operating principle, deduced the mathematical model of the relationship between the loss and the parameters of the optical fiber, and verified the effectiveness of the model through experiments. The operation principle of curvature optical fiber sensor is similar to plane waveguide loss, and the curvature optical fiber sensor can be simplified as a plane waveguide with surface scattering loss. The transmission loss of planar waveguide is mainly from rough surface scattering loss, and the loss is increased with transmission length [37]. Light scattering on upper rough surface of planar waveguide is shown in Fig. 1.

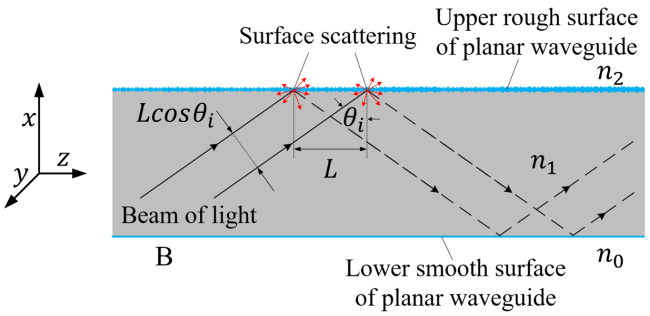

Fig. 1. Light scattering on rough surface of planar waveguide, where n_0, n_1, n_2 is the refractive index of lower cladding, waveguide, upper cladding, respectively, B is the light beam with unit length along Z axis and unit length along Y axis and θ_i is the incident angle.

The incident beam is scattered by the surface, and the transmitted power is expressed in Gaussian units. The power reflected back from the upper surface of the planar waveguide is P_{r21}:

$$P_{r21} = \frac{c}{8\pi} n_1 E_y^2 \cos\theta_i \exp\left[-\left(\frac{4\pi\sigma_{12}}{\lambda_1}\cos\theta_i\right)^2\right] \quad (1)$$

where E_y the electric field component, c is the speed of light, σ_{12} is the mean square deviation of the upper surface contour of the planar waveguide, and λ_1 is the wavelength in the medium of plane wave. So, the attenuation coefficient α is:

$$\alpha = \frac{1}{2}\frac{dP/dz}{P} = 217.2 \times \frac{K^2 \cos^3\theta_i}{\sin\theta_i d_{eff}} \quad (2)$$

where d_{eff} is the effective thickness of the planar waveguide, K is the surface characteristic, and P is the power flow transmitted along the Z axis.

A more visual analysis of the bending loss of the D-shaped POF curvature sensor is shown in Fig. 2.

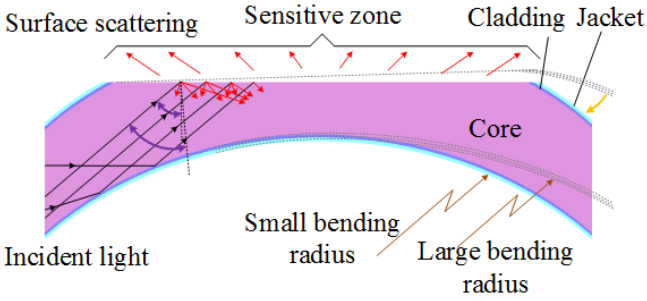

Fig. 2. Relation between curvature and incident angle (positive bending)

When the bend sensitive area of the fiber is located on the convex arc side-polishing area of the plastic optical fiber (which is specified as a positive bend). Assuming that the position of the left side of the fiber is fixed at the incident end, the right side of the fiber segment will change position with increasing bend radius (dashed line in the figure), and the direction of the normal at the sensitive region will be rotated to the dashed position at the same time. It can be found that after the bend radius increases, the angle of incidence θ_i will increase to θ_i' after the light is transmitted to the surface of the sensitive region, i.e., the transmission mode is changed, and some of the higher-order modes are transformed into lower-order modes. Correspondingly, the surface scattering will decrease and the output light intensity will increase.

A section of POF (Jiangxi Dasheng POF Co.Ltd, Jinggangshan, China) was used to fabricate a D-shaped POF sensor, which has a PMMA core of 980 μm diameters , 20 μm thick fluorinated polymeric cladding and 300 μm thick polyethylene jacket. Since the refractive index of the core is higher than that of the cladding, the optical signal propagates primarily in the core, while the jacket provides only mechanical and chemical protection. When the D-shaped POF sensor is bent positively, the amount of optical power leakage in the fiber-sensitive zone varies with the curvature of the fiber [38].

The D-shaped POF sensor is fabricated in the following steps: (1) in order to ensure the exact cutting depth of the plastic fiber, the plastic fiber is fixed with a grooved abrasive tool during cutting, as shown in Fig. 3(a); (2) the POF is cut by hand cutting to remove the jacket, cladding and part of the core above the surface of the abrasive tool, creating a D-shaped profile on

the POF; (3) the D shape profile is finely sanded with thin sandpaper to produce a smooth polished surface, as shown in Fig. 3(b).

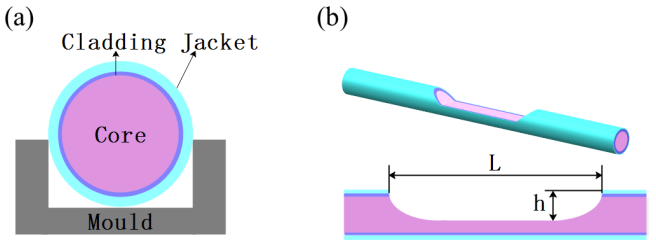

Fig. 3. A schematic diagram of (a) fabricating the D-shaped POF by side-polished method; (b) D-shaped POF, where L is the polish length, h is polish depth.

III. D-SHAPED POF SENSOR CURVATURE EXPERIMENT

The underpinning principle of the proposed sensor is its sensitivity to the curvature variation induced by the breathing. In order to verify this theory, curvature experiments have been carried out by applying bend to the D-shaped POF sensor. A schematic diagram of the setup for curvature sensing is showed in Fig. 4. The light source is a light-emitting diode (LED) IF-E96E with a fixed wavelength of 645 nm, which is connected to the input of the plastic fiber. The D-shaped POF sensor is fixed to an electronic digital angle ruler, with the sensitive zone located at the axis of rotation of the angular ruler so that the sensitive zone is bent positively with a bending angle of β. A power meter (SGOV01, Shenzhen Mateng Technology Co.Ltd) is connected to the output of the plastic fiber to measure the change of output optical power when the sensitive zone is bent. The D-shaped plastic fiber has a side-polish length of 50 mm and a polish depth of about 7 mm.

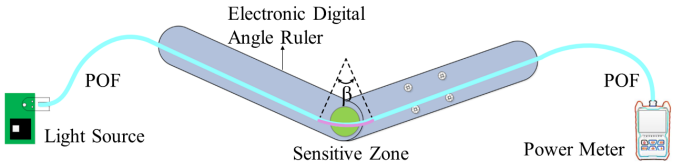

Fig. 4. Schematic diagram of the experimental setup for D-shaped POF sensor curvature experiment.

The angle of D-shaped POF sensor changed on sequential 10° steps from 0°-90°, and the angle values are calibrated by the electronic digital angle ruler. Three independent experiments were conducted, and the results were shown in Fig. 5. It can be seen that the output power decreases monotonically with the increase of the bending angle and the R^2 of the D-shaped POF sensor is 0.9977. The sensor structure has a good response for angular sensing between 0° and 90°. It is noted that the proposed D-shaped POF sensor is a type of intensity modulated optical fiber sensor. The measurement will be affected by the power variation of light source, instability of fiber connection to the light source and detector *etc.*, which is the disadvantage of the intensity measurement-based sensors. In our curvature measurement, due to the above reasons, there are ±50 microwatts power variations in the three independent measurements, which corresponding to 10 degrees deviation. However, in respiration measurement, since human respiration is a periodic signal, the influence of measurement variation due to the above reasons can be eliminated by post-signal processing method, such as low frequency filtering in this paper. In this case, the measurement accuracy for curvature has very limited impact on the measurement accuracy of respiration monitoring.

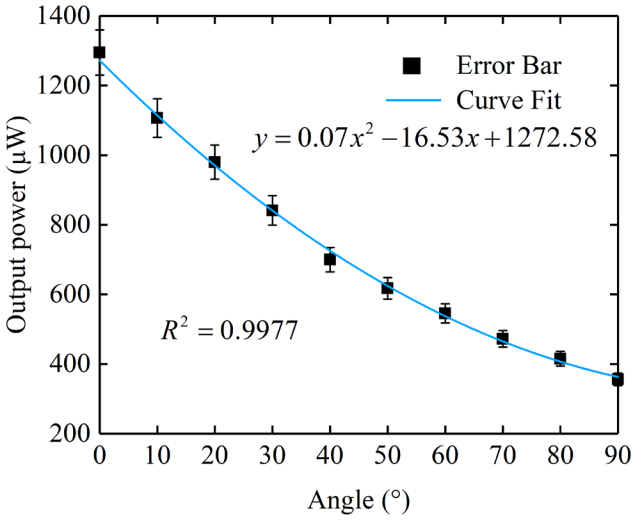

Fig. 5. Output power in response to different degrees of the D-shaped POF sensor.

IV. SYSTEM ARCHITECTURE

The entire respiration monitoring system [shown in Fig. 6(a)] includes light source, D-shaped POF sensor fixed on an elastic belt, optical receiver and a microcontroller (C8051F020). The elastic belt structure is showed in Fig. 6(b), consists of a D-shaped POF sensor, a piece of plastic belt and an elastic fabric. The intensity of the output light was detected by an optical receiver. A program used for the microcontroller was developed based on LABVIEW platform to collect and display the data from the optical receiver with a sampling frequency of 40 Hz. Fig. 6(c) shows the picture of the developed sensor wear around the waist of a volunteer for RR test. The data of respiration variation will be collected when the undulating movement of the abdomen resulting in the curvature of the sensor.

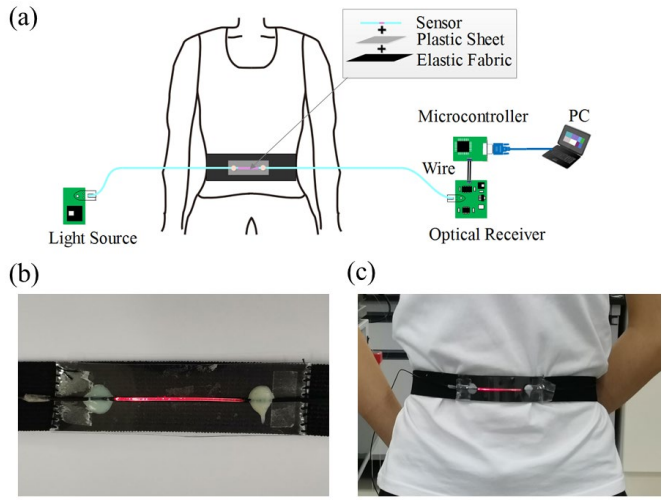

Fig. 6. Experiment setups: (a) System architecture; (b) The elastic belt structure; (c) Wear method.

Fig. 7 shows the circuit and corresponding printed circuit board (PCB) dimensions of the light source and optical receiver. The light source is a red LED IF-E96E (Tempe, AZ, USA), that has a wavelength of 645 nm. A resistor with resistance of 330 Ω was utilized in the circuit with the intent to limit the current in the LED [shown in Fig. 7(a)]. The receiver is used for detecting the light intensity from output of the POF sensor and it is composed of four primary components [shown in Fig. 7(c)], including a photodiode (PD) IF-D91 (Tempe, AZ, USA), a dual op amp amplifier AD706 (Analog Devices), a feedback resistance of 200 kΩ and a feedback capacitance of 0.5 pF. Both the light source and the receiver are powered by 9V dry battery. The +9V voltage was generated by the linear regulator AMS1117-5.0 and the charge pump SGM3204 (SG Micro Corp) to generate +5V and -5V voltages, respectively, to power the AD706. The total cost of the whole system is less than $10.

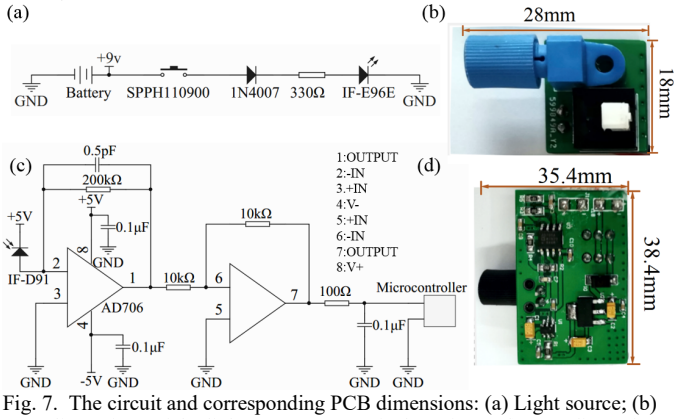

Fig. 7. The circuit and corresponding PCB dimensions: (a) Light source; (b) PCB dimensions of the light source; (c) Optical receiver; (d) PCB dimensions of the optical receiver.

V. Experimental Results and Discussion

A. Respiration signal preprocessing

For monitoring of RR, the elastic fabric with the D-shaped POF sensor is fastened on the abdomen position of a volunteer. A clear respiratory waveform was recorded in Fig. 8(a). By performing a Fast Fourier transform (FFT) on the data [47], the frequency-domain of the respiratory original signal was calculated and presented in Fig. 8(b). The original signal contains baseline interference signals (low-frequency noise), which adversely affects signal analysis and requires preprocessing to eliminate baseline drift and interference. A wavelet transform has time-frequency localization, multi-resolution, decorrelation, and base selection flexibility characteristics [39]. Therefore, the wavelet filtering has a unique advantage over traditional methods in that it can remove noise while retaining the abrupt part of the signal well. A db5 wavelet is used to decompose the original signal in seven layers [40], and the approximation coefficient is zeroed to remove the baseline interference signal. Figures 8(c) and (d) show the time-domain waveform and frequency-domain of the original signal after removing the baseline interference. At the same time, the wavelet transform is used to denoise the breath signal, and the db5 wavelet is used to decompose the original signal in 5 layers, and the detail coefficient is zeroed to remove most of the noise signal. Figures 8(e) and (f) show the time-domain waveform and frequency-domain after the denoising treatment.

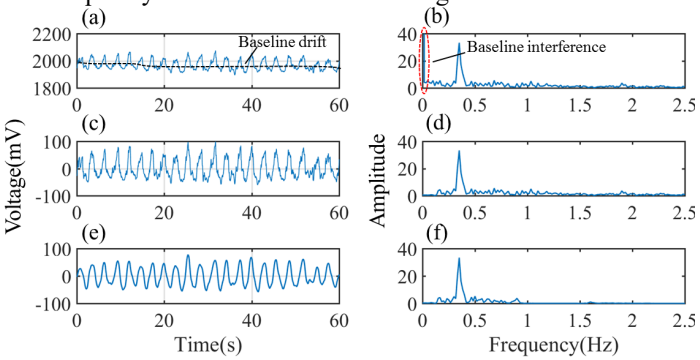

Fig. 8. Respiration signal pre-processing analysis: (a) Time-domain waveform of the original signal; (b) Frequency-domain of the original signal; (c) Time-domain waveform of the interfering signal with baseline removed; (d) Frequency-domain of the baseline interference signal with the baseline removed; (e) The time-domain waveform after the denoising treatment; (f) Frequency-domain after the denoising treatment.

B. RR monitoring

A volunteer (24 years old, female, 156 cm, 42 kg) participated in the experiment of RR monitoring. To demonstrate that a D-shaped POF sensor is capable of accurately measuring RR under various human movement conditions. The volunteer performed three groups of experiments to measure RR in resting, walking, and running situations. Fig. 9 presents the experimental results of the three groups of experiments. Figures 9(a-c) show the time-domain waveforms of the original signals measured in the resting, walking, and running states, respectively. It can be seen that there is a lot of noise in the time-domain waveform of the motion (walking and running) compared to the resting state. This is due to the motion noise interference generated during human movement, which causes the respiratory signal waveform to be superimposed with motion interference noise. At the same time, comparing the time-domain waveform in the walking and running state, it can be seen that the more intense the motion, the more severe the motion noise interference. Figures 9(d-f) show the time-domain waveforms of the respiratory signals after signal preprocessing in the resting, walking, and running states, respectively. It can be seen that the original signal measured in the exercise state can recover a smooth and clear respiratory signal after pre-processing. Figures 9(g-i) show the frequency-domain of the three states (resting, walking and running), respectively. It can be seen that their frequencies are 0.28 Hz, 0.35 Hz, and 0.43 Hz, respectively. The normal respiratory frequency of the human body is between 0.2-0.4 Hz [18], and the RR will increase during exercise, and the respiratory frequency is 0.43 Hz when running, which is a normal physiological phenomenon and also basic knowledge in the medical field. Therefore, the D-shaped POF sensor can realize the measurement of the RR of the human body in different exercise states.

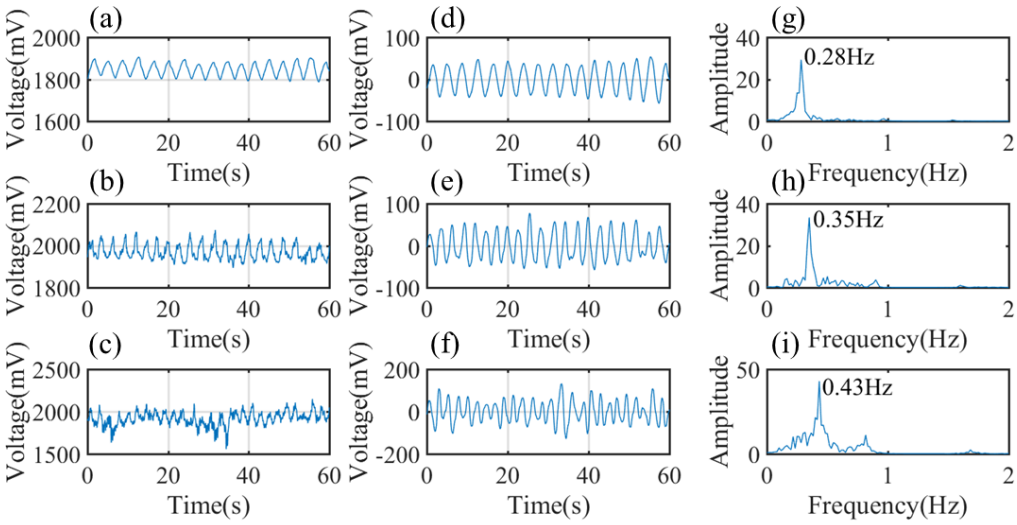

Fig. 9. (a-c) Time-domain waveform of the original signal at resting, walking and running, respectively; (d-f) The corresponding time-domain waveform of the respiratory signal after signal and processing; (g-i) The corresponding frequency-domain of the respiratory signal.

The most common method used classically to analyze and process stable signals is the Fourier transform, but the shortcoming of the Fourier transform is that it decomposes the signal into different frequency components as a whole, and it does not reveal when a certain frequency component occurs and how it changes over time. Therefore, we introduce scalogram to describe the time-frequency distribution of non-stationary signals. If a bilinear time-scale generalized distribution function $\Omega_x(t,a)$ has time and scale invariance for the affine transformation, i.e. [41],

$$\Omega_{x_{a'b'}}(t,a)=\Omega_x\left(\frac{t-b'}{a'},\frac{a}{a'}\right) \tag{3}$$

then there is

$$\Omega_x(t,a;\Pi)=\int_{-\infty}^{\infty}\int_{-\infty}^{\infty}\Pi\left(\frac{s-t}{a},a\xi\right)W_x(s,\xi)dsd\xi \tag{4}$$

where t, b', and s are time variables, a and a' are scale variables, $\Pi(t, v)$ is an arbitrary smooth function, $W_x(s, \xi)$ is the Wigner-Ville transformation of the signal $x(t)$, ξ and v are frequency variables. Eq. (4) shows that the whole of the time-scale distribution defines the affine time-frequency distribution. The scalogram is an affine time-frequency distribution, which can actually be used as a smoothed form of the Wigner-Ville distribution:

$$|T_x(t,a,\psi)|^2=\int_{-\infty}^{\infty}\int_{-\infty}^{\infty}W_x(s,\xi)W_\psi\left(\frac{s-t}{a},a\zeta\right)dsd\zeta \tag{5}$$

Thus, the scale map is the affine class distribution corresponding to the smoothing function $\Pi(t,v)=W_\psi\left(\frac{s-t}{a},a\zeta\right)$.

Fig. 10 represents the time-domain waveform of the unstable respiratory signal and its time-frequency distribution. Figures 10(a) and (b) show the time-domain waveforms of pauses in respiration and changes in respiration from fast to slow, respectively. Applying the scalogram, the time-frequency distributions, as shown in Figures 10(c) and (d). Fig. 10(c) shows that the participant had a RR of 0.3 Hz at 0-35 s and respiratory pauses at 35-60 s, which is consistent with the time-domain waveform of Fig. 10(a). Fig. 10(d) shows that the participant's RR at 0-15 s was 0.8 Hz; 15-35 s was approximately 0.55 Hz; and 35-60 s was approximately 0.35 Hz, consistent with the time-domain waveform of Fig. 10(b). The scale diagram can effectively analyze the instantaneous RR of the respiratory signal, which can be used to help medical personnel monitor the patient's obstructive sleep apnea and respiratory disorders.

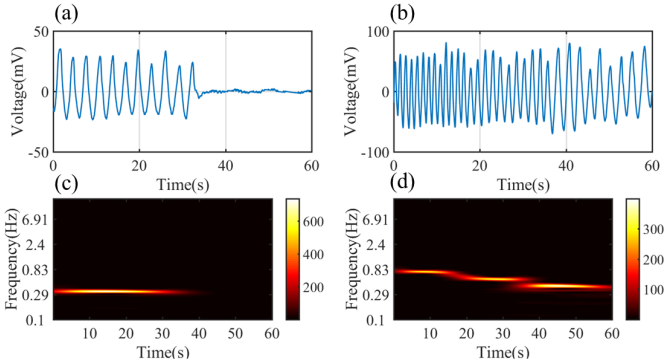

Fig. 10. Analysis of unsteady respiratory signals: (a) Time-domain waveform of pause signal; (b)Time-domain waveform of respiratory change signal from fast to slow; (c)Time-frequency distribution of pause signal; (d) Time-frequency distribution of respiratory change signal from fast to slow.

To show the applicability of the POF sensor in RR measurement an experiment with 6 healthy participants (3 females and 3 males) was carried out. Figures 11(a) and 11(b) show the time-domain and frequency-domain waveforms of the normal respiratory signals of the 6 participants. As seen in Fig. 11(b), the RR of all six participants was within the range of the normal human RR. Above results demonstrated that the proposed POF wearable devices can be used to human RR monitoring among different individuals.

Table I compares the performance of the proposed respiratory monitoring system with some of the latest reported systems. Parameters such as the type of sensors used in these systems, sensor locations and their fabrication process complexity are listed in the table. Compared with these latest systems, the sensor fabrication process is simpler, the cost of the whole system is lower, and the size is smaller, owing to the use of a D-shaped POF sensor with a low-cost light source and optical receiver.

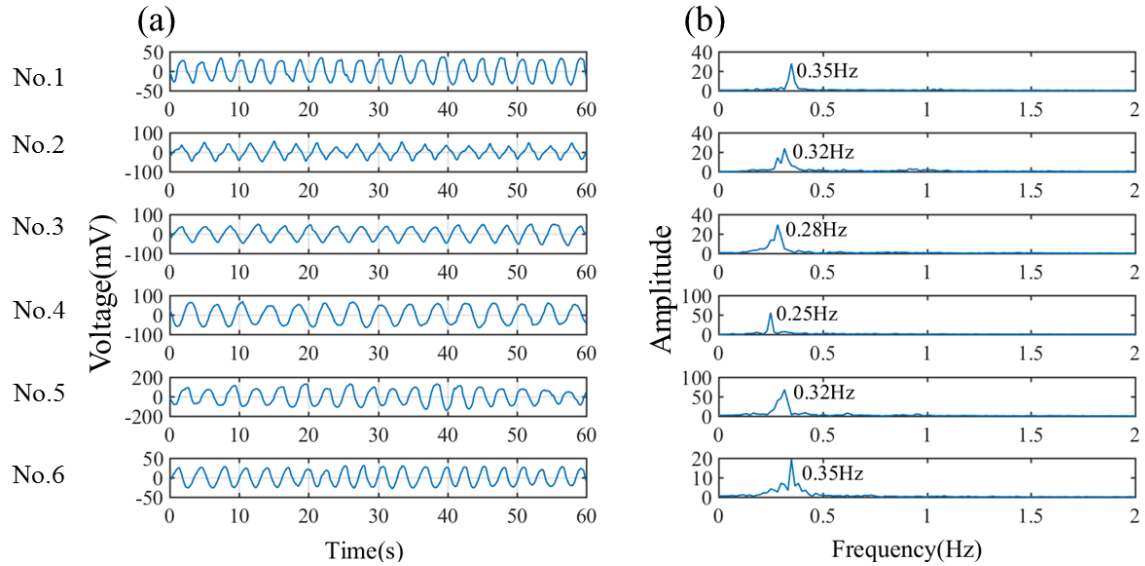

Fig. 11. (a) Time-domain waveforms of the respiratory signals of the six participants; (b) Frequency-domain of the respiratory signals of the 6 participants.

TABLE I
COMPARISON TABLE

Sensor Type	Sensor Location	Sensor Fabrication	Size	Cost	Ref.
Humidity	Nose (below)	Complex	Small (length is 4 mm)	High	[42] (2020)
Capacitive	Distance from chest (20 cm height)	Less complex	Diameter φ is 250 mm (PCB)	Medium	[43] (2020)
Piezoelectric	Chest (shirt or belt)	Complex	75×15 mm	Low	[44] (2020)
Camera	Distance from participant (100 cm away)	-	-	High	[45] (2020)
Optical fiber MZI	Mat	Complex	300×300 mm	High	[46] (2020)
SMS structure	Abdomen(belt)	Simple	220×80 mm (light source) and 40×60 mm (PD)	High	[47] (2020)
Micro-bend fiber	Mat	Simple	210×297 mm	Medium	[48] (2019)
Hetero-core fiber	Lower side of the left chest(shirt)	Less complex	60×85 mm	Low	[49] (2018)
D-shaped POF	Abdomen(belt)	Simple	28×18 mm (light source) and 35.4×38.4 mm (optical receiver)	Low	This work

VI. CONCLUSION

In conclusion, a wearable respiratory monitoring device based on a D-shaped POF sensor was proposed and experimentally demonstrated. The curvature characteristics of the POF sensor show that it has good response to angular variation between 0° and 90°, which is an idea sensor for low-cost monitoring of RR. Both the regular and irregular RR can be achieved by wavelet decomposition, FFT and scalogram methods. In addition, the device has good anti-interference characteristics, which can be used to monitor a person's RR under different exercise states (resting, walking and running). The wearable design of the system is easy to wear on the human abdomen for long-term continuous monitoring of the respiratory signals. The advantages of the system are low cost, compactness and simple design. At the same time, using the proposed Wavelet noise reduction technology, the influence of body movement on the sensor response can be eliminated. The proposed system provides a simple and inexpensive optical solution for wearable respiratory monitoring.

REFERENCES

[1] J. X. Dai, X. Guan, H. R. Zhao, S. Liu, T. Fei, and T. Zhang, "In situ preparation of porous humidity sensitive composite via a one-stone-two-birds strategy," *Sensors and Actuators B: Chemical*, vol. 316, pp. 128-159, Apr. 2020.

[2] S. Kort, M. Brusse-Keizer, J. W. Gerritsen, H. Schouwink, E. Citgez, F. Jongh, J. Maten, S. Samii, M. Bogart, and J. Palen, "Improving lung cancer diagnosis by combining exhaled-breath data and clinical parameters," *ERJ Open Research*, vol. 6, no. 1, Jan. 2020.

[3] N. Dharmawardana, C. Woods, D. I. Watson, R. Yazbeck, and E. H. Ooi, "A review of breath analysis techniques in head and neck cancer," *Oral oncology*, vol. 104, p. 104654, Mar. 2020.

[4] A. Tiele, A. Wicaksono, E. Daulton, E. Ifeachor, V. Eyre, S. Clarke, L. Timings, S. Pearson, J. A. Covington, and X. Z. Li, "Breath-based non-invasive diagnosis of Alzheimer's disease: a pilot study," *Journal of Breath Research*, vol. 14, no. 2, p. 026003, 2020.

[5] W. Daw, R. Kaur, M. Delaney, and H. Elphick, "Respiratory rate is an early predictor of clinical deterioration in children," *Pediatr Pulmonol*, vol. 55, no. 8, pp. 2041-2049, May. 2020.

[6] P. C. Loughlin, F. Sebat, and J. G. Kellet, "Respiratory rate: The forgotten vital sign—make it count," *Joint Commission Journal on Quality and Patient Safety*, vol. 44, no. 8, pp. 494-499, 2018.

[7] J. Kellett, and F. Sebat, "Make vital signs great again - A call for action", *European journal of internal medicine*, vol. 45, pp. 13-19, 2017.

[8] M. A. Cretikos, R. Bellomo, K. Hillman, J. Chen, S. Finfer, and A. Flabouris, "Respiratory rate: The neglected vital sign," *The Medical journal of Australia*, vol. 188, no. 11, pp. 657–659, Jun. 2008.

[9] J. E. Lee, and S. K. Yoo, "Radar-based detection of respiration rate with adaptive harmonic quefrency selection," *Sensors*, vol. 20, no. 6, p. 1607, Mar. 2020.

[10] M. H. Hu, G. T. Zhai, D. Li, Y. Z. Fan, X. H. Chen, and X. K. Yang, "Synergetic use of thermal and visible imaging techniques for contactless and unobtrusive breathing measurement," *Journal of Biomedical Optics*, vol. 22, no. 3, p. 036006, Mar. 2017.

[11] M. A. Hassan, A. S. Malik, D. Fofi, N. Saad, B. Karasfi, Y. S. Ali, and F. Meriaudeau, ''Heart rate estimation using facial video: A review,'' *Biomedical Signal Processing and Control*, no. C, vol. 38, pp. 346-360, Sep. 2017.

[12] P. Jagadev, and L. I. Giri, "Human respiration monitoring using infrared thermography and artificial intelligence," *Biomedical Physics & Engineering Express*, vol. 6, no. 3, p. 035007, 2020.

[13] L. Y. Ma, R. H. Wu, A. Patil, S. H. Zhu, Z. H. Meng, H. Q. Meng, C. Hou, Y. F. Zhang, Q. Liu, R. Yu, J. Wang, N. Lin, and X. Y. Liu, "Full-textile wireless flexible humidity sensor for human physiological monitoring," *Advanced Functional Materials*, vol. 29, no. 43, p. 1904549, Jul. 2019.

[14] D. X. Qiu, Y. C. Chu, H. X. Zeng, H. H. Xu, and G. Dan, "Stretchable MoS_2 electromechanical sensors with ultrahigh sensitivity and large detection range for skin-on monitoring," *ACS Applied Materials & Interfaces*, vol. 11, no. 40, pp. 37035-37042, Sep. 2019.

[15] S. W. Chen, N. Wu, L. Ma, S. Z. Lin, F. Yuan, Z. S. Xu, W. B. Li, B. Wang, and J. Zhou, "Non-contract heartbeat and respiration monitoring based on hollow-microstructure self-powered pressure sensor," *ACS Applied Materials & Interfaces*, vol. 10, no. 4, pp. 3660-3667, Jan. 2018.

[16] F. X. Wang, S. H. Zhang, Y. L. Zhang, Q. H. Lin, Y. Chen, D. F. Zhu, L. N. Sun, and T. Chen, "Facile fabrication of a self-healing temperature-sensitive sensor based on ionogels and its application in detection human breath," *Nanomaterials*, vol. 9, no. 3, p. 343, Mar. 2019.

[17] T. Sirkis, Y. Biederman, S. Agdarov, Y. Beiderman, and Z. Zalevsky, "Fiber sensor for non-contact estimation of vital bio-signs," *Optics Communications*, vol. 391, pp. 63-67, Jan. 2017.

[18] R. H. Wang, J. Zhao, Y. Sun, H. Yu, N. Zhou, H. X. Zhang, and D. G. Jia, "Wearable respiration monitoring using an in-line few-mode fiber Mach-Zehnder interferometric sensor," *Biomedical optics express*, vol. 11, no. 1, pp. 316-329, Jan. 2020.

[19] X. Li, D. Liu, R. Kumar, W. P. Ng, Y. Q. Fu, J. Yuan, C. Yu, Y. Wu, G. Zhou, G. Farrell, Y. Semenova, and Q. Wu, "A simple optical fiber interferometer based breathing sensor", *Measurement Science and Technology*, vol. 28, no. 3, 2017.

[20] C. Massaroni, M. Zaltieri, D. Lo Presti, A. Nicolò, D. Tosi, and E. Schena, "Fiber Bragg Grating sensors for cardiorespiratory monitoring: A Review," *IEEE Sensors Journal*, 2020.

[21] A. Issatayeva, A. Beisenova, D. Tosi, and C. Molardi, "Fiber-Optic Based Smart Textiles for Real-Time Monitoring of Breathing Rate," *Sensors*, vol. 20, no. 12, p. 3408, Jun. 2020.

[22] K. Li, L. Xia, H. Yi, S. Y. Li, Y. Wu, and Y. M. Song, "Optical active fiber sensing technique based on the lasing wavelength demodulation for monitoring the human respiration and pulse," *Sensor and Actuators A: Physical*, vol. 296, pp. 45-51, Jul. 2019.

[23] S. P. Morgan, S. Korposh, L. Liu, F. U. Hernandez, R. Correia, A. Norris, R Sinha, B. R. Hayes-Gill, S.A. Piletsky, F. Canfarotta, E. V. Piletska, and F. Grillo, "Optical fiber sensors for monitoring in critical care," *IEEE Engineering in Medicine and Biology Society*, pp. 1139-1143, 2019.

[24] H. F. Hu, S. J. Sun, R. Q. Lv, and Y. Zao, "Design and experiment of an optical fiber micro bend sensor for respiration monitoring," *Sensors and Actuators A: Physical*, vol. 251, pp. 126-133, 2016.

[25] M. Nishyama, M. Miyamoto, and K. Watanabe, "Respiration and body movement analysis during sleep in bed using hetero-core fiber optic pressure sensors without constraint to human activity," *Journal of Biomedical Optics*, vol. 16, no. 1, p. 017002, Jan. 2011.

[26] A. G. Leal-Junior, C. R. Diaz, M. F. Jiménez, C. Leitão, C. Marques, M. J. Pontes, and A. Frizera, "Polymer optical fiber-based sensor system for smart walker instrumentation and health assessment," *IEEE Sensors Journal*, vol. 19, no. 2, pp. 567-574, 2019.

[27] M. Krehel, M. Schmid, R. M. Rossi, L. F. Boesel, G. L. Bona, and L. J. Scherer, "An optical fibre-based sensor for respiratory monitoring," *Sensors*, vol. 14, no. 7, pp. 13088-13101, Jul. 2014.

[28] W. Zheng, X. M. Tao, B. Zhu, G. F. Wang, and C. Y. Hui, "Fabrication and evaluation of a notched polymer optical fiber fabric strain sensor and its application in human respiration monitoring," *Textile Research Journal*, vol. 84, no. 17, pp. 1791-1802, Apr. 2014.

[29] D. Sartiano, and S. Sales, "Low cost plastic optical fiber pressure sensor embedded in mattress for vital signal monitoring," *Sensors*, vol. 17, no. 12, Dec. 2017.

[30] A. Aitkulov, and D. Tosi, "Optical fiber sensor based on plastic optical fiber and smartphone for measurement of the breathing rate," *IEEE Sensors Journal*, vol. 19, no. 9, pp. 3282-3287, May. 2019.

[31] A. G. Leal-Junior, C. R. Díaz, C. Leitão, M. J. Pontes, C. Marques, and A. Frizera, "Polymer optical fiber-based sensor for simultaneous measurement of breath and heart rate under dynamic movements," *Optics and Laser Technology*, vol. 109, pp. 429–436, 2019.

[32] L. Bilro, N. Alberto, J. L. Pinto, and R. Nogueira, "Optical sensors based on plastic fibers," *Sensors*, vol. 12, no. 9, pp. 12184-12207, Sep. 2012.

[33] K. Peters, "Polymer optical fiber sensors—a review," *Smart Materials and Structures*, vol. 20, no. 1, pp. 013002-1–013002-17, 2011.

[34] K. Bhowmik, G. Peng, E. Ambikairajah, V. Lovric, W. R. Walsh, B. G. Prusty, and G. Rajan, "Intrinsic high-sensitivity sensors based on etched single-mode polymer optical fibers," *IEEE Photonics Technology Letters*, vol. 27, no. 6, pp. 604-607, 2015.

[35] A. Rezende, C. Alves, I. Marques, M. A. Silva, and E. Naves, "Polymer optical fiber goniometer: A new portable, low cost and reliable sensor for joint analysis," *Sensors (Basel)*, vol. 18, no. 12, p. 4293, Dec. 2018.

[36] L. Bilro, J. G. Oliveira, J. L. Pinto, and R. N. Nogueira, "A reliable low-cost wireless and wearable gait monitoring system based on a plastic optical fibre sensor," *Measurement Science and Technology*, vol. 22, no. 4, p. 045801, Mar. 2011.

[37] R. Q. Liu, Z. Fu, Y. Z. Zhao, Q. X. Cao, and S. G. Wang "Operation principle of a bend enhanced curvature optical fiber sensor," in *2006 IEEE/RSJ International Conference on Intelligent Robots and Systems*, Beijing, China, 2006, pp. 1966-1971.

[38] A. G. Leal Junior, A. Frizera, and M. J. Pontes, "Analytical model for a polymer optical fiber under dynamic bending," *Optics and Laser Technology*, vol. 93, pp. 92-98, 2017.

[39] D. B. Percival, and A. T. Walden, *Wavelet Methods for Time Series Analysis (Cambridge Series in Statistical and Probabilistic Mathematics).* Cambridge, UK: Cambridge UP, 2000, pp. 1-19.

[40] D. B. Percival, and A. T. Walden, *Wavelet Methods for Time Series Analysis (Cambridge Series in Statistical and Probabilistic Mathematics).* Cambridge, UK: Cambridge UP, 2000, pp. 105-117.

[41] P. Flandrin, and P. Goncalvès, "Geometry of affine time–frequency distributions," *Applied and Computational Harmonic Analysis*, vol. 3, no. 1, pp. 10-39, 1996.

[42] G. Wang, Y. zhang, H. Yang, W. Wang, Y. Z. Dai, L. G. Niu, C. Lv, H. Xia, and T. Liu, "Fast-response humidity sensor based on laser printing for respiration monitoring," *RSC Advances*, vol. 10, no. 15, pp. 8910-8916, 2020.

[43] R. Kusche, F. John, M. Cimdins, and H. Hellbrück, "Contact-free biosignal acquisition via capacitive and ultrasonic sensors," *IEEE Access*, vol. 8, pp. 95629-95641, 2020.

[44] A. Panahi, A. Hassanzadeh, and A. Moulavi, "Design of a low cost, double triangle, piezoelectric sensor for respiratory monitoring applications," *Sensing and Bio-Sensing Research*, vol. 30, p. 100378, 2020.

[45] P. Jakkaew, and T. Onoye, "Non-contact respiration monitoring and body movements detection for sleep using thermal imaging," *Sensors*, vol. 20, p. 6307, Nov. 2020.

[46] S. Wang, X. Ni, L. Li, J. Wang, Q. Liu, Z. Yan, L. Zhang, and Q. Sun, "Noninvasive monitoring of vital signs based on highly sensitive fiber optic mattress," *IEEE Sensors Journal*, vol. 20, no. 11, pp. 6182-6190, 2020.

[47] Y. N. Pang, B. Liu, J. Liu, S. P. Wan, T. Wu, X. D. He, J. Yuan, X. Zhou, K. Long, and Q. Wu, "Wearable optical fiber sensor based on a bend singlemode-multimode-singlemode fiber structure for respiration monitoring", *IEEE Sensors Journal*, 2020, 10.1109/JSEN.2020.3032646
[48] Y. Zhang, Z. Chen, and H. I. Hee, "Noninvasive Measurement of Heart Rate and Respiratory Rate for Perioperative Infants," *Journal of Lightwave Technology*, vol. 37, no. 11, pp. 2807-2814, 2019.
[49] Y. Koyama, M. Nishiyama, and K. Watanabe, "Smart textile using hetero-core optical fiber for heartbeat and respiration monitoring," *IEEE Sensors Journal*, vol. 18, no. 15, pp. 6175-6180, 2018.

Yu-Lin Wang received the B.S. degree from Wuhan Polytechnic University in 2019. She is currently pursuing the M.S. degree in optical engineering with Nanchang Hangkong University. Her current research interests include optical fiber sensing and signal processing.

Bin Liu received his B.S. and Ph.D. degree from Sun Yat-sen University, China. Dr. Liu is an associate Professor with Key Laboratory of Opto-Electronic Information Science and Technology of Jiangxi Province, Nanchang Hangkong University, Nanchang 330063, China. His research interests include optical fiber sensing and signal processing, nanofiber, microsphere sensors for bio-chemical sensing, nonlinear fiber optics, surface plasmon resonant.

Yi-Neng Pang received the B.S. degree from Hunan Institute of Engineering in 2017. He is currently pursuing the M.S. degree in optical engineering with Nanchang Hangkong University. His current research interests include optical fiber sensing and signal processing.

Juan Liu received her Ph.D. degree from Beijing Normal University, China. She is a lecture with Key Laboratory of Opto-Electronic Information Science and Technology of Jiangxi Province, Nanchang Hangkong University, China. Her main research interest is fiber optic sensing.

Jiu-Lin Shi received Ph.D. degree from Huazhong University of Science and Technology, Wuhan, China. He is currently a Professor with the Key Laboratory of Opto-Electronic Information Science and Technology of Jiangxi Province, Nanchang Hangkong University, China. His current research interests include optical testing.

Sheng-Peng Wan received the B.S. and Ph.D. degrees from University of Electronic and Technology of China. He is a professor with Key Laboratory of Opto-Electronic Information Science and Technology of Jiangxi Province, Nanchang Hangkong University, China. His main research interest is fiber optic sensing.

Xing-Dao He was born in Jingan, China, in 1963. He received the Ph.D. degree in optics from Beijing Normal University, Beijing, China, in 2005. He is currently a Professor with Key Laboratory of Opto-Electronic Information Science and Technology of Jiangxi Province, Nanchang Hangkong University, China. His current research interests include light scattering spectroscopy, optical holography, and information processing.

Jinhui Yuan received the Ph.D. degree in physical electronics from Beijing University of Posts and Telecommunications (BUPT), Beijing, China, in 2011. He is currently a Professor at the Department of computer and communication engineering, University of Science and Technology Beijing (USTB). He was selected as a Hong Kong Scholar at the Photonics Research Centre, Department of Electronic and Information Engineering, The Hong Kong Polytechnic University, in 2013. His current research interests include photonic crystal fibers, silicon waveguide, and optical fiber devices. He is the Senior Members of the IEEE and OSA. He has published over 200 papers in the academic journals and conferences.

Qiang Wu received the B.S. and Ph.D. degrees from Beijing Normal University and Beijing University of Posts and Telecommunications, Beijing, China, in 1996 and 2004, respectively. From 2004 to 2006, he worked as a Senior Research Associate in City University of Hong Kong. From 2006 to 2008, he took up a research associate post in Heriot-Watt University, Edinburgh, U.K. From 2008 to 2014, he worked as a Stokes Lecturer at Photonics Research Centre, Dublin Institute of Technology, Ireland. He is with Faculty of Engineering and Environment, Northumbria University, Newcastle Upon Tyne, United Kingdom; Key Laboratory of Opto-Electronic Information Science and Technology of Jiangxi Province, Nanchang Hangkong University, Nanchang 330063, China. His research interests include optical fiber interferometers for novel fiber optical couplers and sensors, nanofiber, microsphere sensors for bio-chemical sensing, the design and fabrication of fiber Bragg grating devices and their applications for sensing, nonlinear fibre optics, surface plasmon resonant and surface acoustic wave sensors. He has over 200 journal publications in the area of photonics and holds 3 invention patents. He is an Editorial Board Member of Scientific Reports, an Associate Editor for IEEE Sensors Journal and an Academic Editor for Journal of Sensors.